JOURNAL OF VIROLOGY, Jan. 2005, p. 1113–1124 Vol. 79, No. 2
0022-538X/05/$08.00+0 doi:10.1128/JVI.79.2.1113–1124.2005

Infection of Ciliated Cells by Human Parainfluenza Virus Type 3 in an In Vitro Model of Human Airway Epithelium

Liqun Zhang,[1] Alexander Bukreyev,[2] Catherine I. Thompson,[1] Brandy Watson,[2] Mark E. Peeples,[3,4] Peter L. Collins,[2] and Raymond J. Pickles[1,5]*

Cystic Fibrosis/Pulmonary Research and Treatment Center,[1] and Department of Microbiology and Immunology,[5] University of North Carolina at Chapel Hill, Chapel Hill, North Carolina; Respiratory Viruses Section, National Institute of Allergy and Infectious Diseases, National Institutes of Health, Bethesda, Maryland[2]; and Center for Vaccines and Immunity, Columbus Children's Research Institute,[3] and Department of Pediatrics, The Ohio State University,[4] Columbus, Ohio

Received 5 July 2004/Accepted 2 August 2004

We constructed a human recombinant parainfluenza virus type 3 (rPIV3) that expresses enhanced green fluorescent protein (GFP) and used this virus, rgPIV3, to characterize PIV3 infection of an established in vitro model of human pseudostratified mucociliary airway epithelium (HAE). The apical surface of HAE was highly susceptible to rgPIV3 infection, whereas only occasional cells were infected when virus was applied to the basolateral surface. Infection involved exclusively ciliated epithelial cells. There was little evidence of virus-mediated cytopathology and no spread of the virus beyond the ciliated cell types. Infection of ciliated cells by rgPIV3 was sensitive to a neuraminidase specific for α2-6-linked sialic acid residues, but not to a neuraminidase that cleaves α2-3- and α2-8-linked sialic acid residues. This provided evidence that rgPIV3 utilizes α2-6-linked sialic acid residues for initiating infection, a specificity also described for human influenza viruses. The PIV3 fusion (F) glycoprotein was trafficked exclusively to the apical surface of ciliated cells, which also was the site of release of progeny virus. F glycoprotein localized predominately to the membranes of the cilial shafts, suggesting that progeny viruses may bud from cilia per se. The polarized trafficking of F glycoprotein to the apical surface also likely restricts its interaction with neighboring cells and could account for the observed lack of cell-cell fusion. HAE derived from cystic fibrosis patients was not more susceptible to rgPIV3 infection but did exhibit limited spread of virus due to impaired movement of lumenal secretions due to compromised function of the cilia.

The human parainfluenza viruses (PIV) are common human respiratory tract pathogens. Four serotypes of human PIV have been identified, with serotypes 1, 2, and 3 being the most significant for human disease. Indeed, PIV type 3 (PIV3) is second only to human respiratory syncytial virus (RSV) as the most common cause of serious respiratory tract disease in infants and children. Approximately 60% of children have been infected with PIV3 by 2 years of age, and bronchiolitis and/or pneumonia can occur in 10 to 30% of those infected, especially those that are immunocompromised or have chronic respiratory or cardiac disease. PIV3 infects and causes disease in the respiratory tract but does not spread significantly beyond that site. Both innate and adaptive immune responses contribute to clearing PIV3 infection and to the development of resistance to subsequent reinfection. However, protection can be incomplete and reinfection is common (9).

PIV3 is a member of the genus *Respirovirus*, subfamily *Paramyxovirinae*, family *Paramyxoviridae*. Like other paramyxoviruses, it is an enveloped nonsegmented negative-strand RNA virus that enters the infected cell by fusion at the plasma membrane, replicates in the cytoplasm, and buds at the plasma membrane. The viral nucleoprotein (N), phosphoprotein (P), and large RNA polymerase (L) protein, together with the viral genome, form the viral nucleocapsid, while the matrix (M) protein is located between the nucleocapsid and the lipid envelope and mediates viral maturation and budding. The hemagglutinin-neuraminidase (HN) and F transmembrane surface glycoproteins mediate viral attachment and fusion and are the neutralization and major protective antigens (9, 26).

PIV3 attaches to target cells via the HN protein and fuses with the plasma membrane in a pH-independent fusion process mediated by the F glycoprotein acting in concert with HN (23, 27, 36, 49, 52). The HN protein attaches to *N*-acetylneuraminic (sialic) acid residues on cell surface glycoconjugates, and sialoglycoproteins and glycolipids have been reported to facilitate PIV attachment (31, 32). Using African green monkey kidney fibroblasts (CV-1 cells), it has been reported that PIV3 attached to a specific sialic acid-containing receptor(s) but did not indiscriminately bind to sialic acid-containing molecules; however, no attempt to characterize the sialic acid linkage or the glycoconjugates bearing the sialic acid was attempted in that study (29). In a non-cell-based assay, both PIV1 and PIV3 bound to purified neolacto-series gangliosides through an interaction with α2-3-linked sialic acid residues on the blood group I antigen (48). Another study used a human transformed alveolar type II cell line (A549) to show that an interaction of PIV3 with sialic acid residues only accounted for ~50% of the infection; the remainder appeared to be due to an interaction of PIV3 with cell surface heparan sulfate (HS) moieties (4). HS has been reported as an attachment receptor for several diverse viruses known to infect the lung, i.e., adenovirus (Ad), adeno-associated virus, and RSV (13, 14, 18, 21, 25, 47).

While the tropism of human PIV for human lung epithelium

* Corresponding author. Mailing address: CF/Pulmonary Research and Treatment Center, 7021 Thurston Bowles, University of North Carolina at Chapel Hill, Chapel Hill, NC 27599-7248. Phone: (919) 966-7044. Fax: (919) 966-5178. E-mail: branston@med.unc.edu.

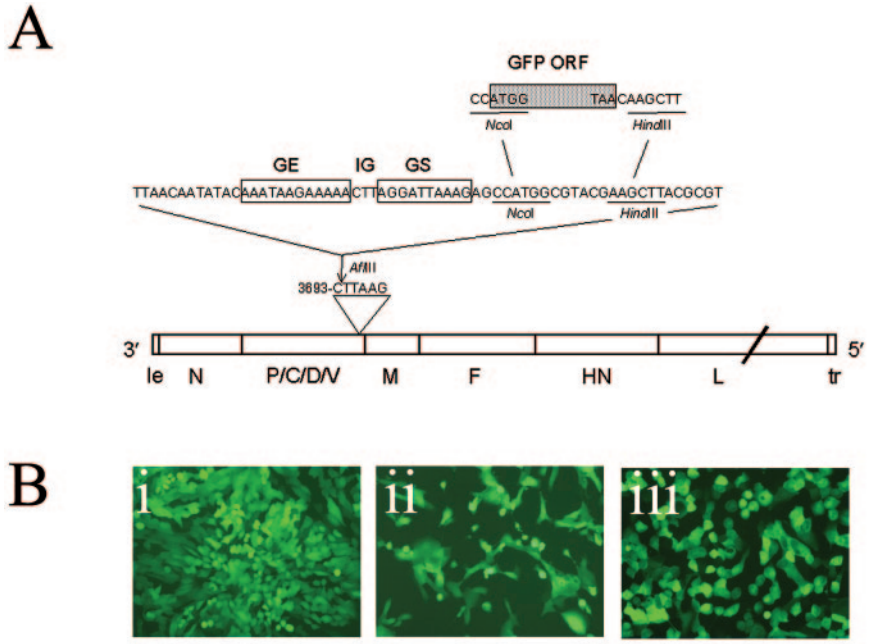

FIG. 1. Recombinant PIV3 expressing enhanced GFP from an added reporter gene (rgPIV3). (A) The coding sequence for GFP was inserted into the downstream noncoding region of the P/C/D/V gene. Nucleotides 3693 to 3698 of the PIV3 genome were modified into an AflIII site, which was used to accept an insert that contained PIV3 gene-end (GE), intergenic (IG), and gene-start (GS) signals, followed by NcoI and HindIII sites. These latter sites were used to accept an NcoI-HindIII fragment containing the open reading frame for enhanced GFP (shaded rectangle, with the ATG and TAA initiation and termination codons indicated). (B) Fluorescent photomicrographs showing the intracellular expression of GFP in cell culture at 36 h following rgPIV3 infection of HEp-2 cells (i), A549 cells (ii), or nonpolarized, PD primary airway epithelial cells (iii). Original magnification, ×10.

is well known, few studies have characterized how these viruses interact with the ciliated airway epithelium derived from human airways. Since ciliated epithelium is present in the nasal and sinus cavities, as well as the proximal and distal conducting airways, infection of these cell types could be directly involved in the pathogenesis of croup, bronchitis, and bronchiolitis. Using polarized A549 cells as a model of airway epithelium, Bose et al. showed that PIV3 infection and subsequent viral shedding occurred predominately, though not exclusively, at the apical surface (5). The reported basolateral shedding of PIV3 is inconsistent with the typical lack of viremia and systemic spread of PIV3, although this may be limited by the presence of serum neutralizing antibodies. However, monolayer cultures of A549 cells may not reflect the morphology of the polarized epithelium of the human conducting airways.

To determine the characteristics of PIV3 infection of cells that resemble the morphological phenotype of the human respiratory ciliated epithelium, we have generated a recombinant PIV3 that expresses green fluorescent protein (GFP) (rgPIV3) and monitored infection of a well-characterized in vitro model of human airway epithelium (HAE) (41). This involves primary culture of human airway epithelial cells that are grown at an air-liquid interface (ALI) to generate a differentiated, pseudostratified, mucociliary epithelium that closely models human conducting airway epithelium in vivo. We previously reported the use of this model to characterize infection by a recombinant, GFP-expressing RSV (rgRSV), a member of the distinct *Pneumovirinae* subfamily, and showed that rgRSV infection was specific for human ciliated cells and occurred without characteristic syncytium formation (53).

MATERIALS AND METHODS

Viruses. For the construction of rgPIV3 (based on the JS strain), a 720-bp cDNA encoding the enhanced GFP of *Renilla reniformes* (Life Technologies, Gaithersburg, Md.) was modified by PCR to be flanked by PIV3 gene-start and gene-end sequences (Fig. 1A). This was accomplished with the primers GAAT TCACC*ATGG*TGAGTAA and TGTAC*AAGCTT*GTTAAACCCATTCGTGT AAGG as forward and reverse primers, respectively. In the forward primer, an NcoI restriction site is italicized, and the beginning of the GFP open reading frame is underlined. In the reverse primer, a HindIII restriction site is italicized, and the complement of the end of the GFP open reading frame (ORF) is underlined. The PCR product was digested with NcoI and HindIII and inserted into the NcoI-HindIII window of a subclone representing the PmlI-to-BamHI restriction fragment of the PIV3 strain JS antigenomic cDNA. This subclone includes the downstream end of the N gene, the P/C/D/V gene, and the upstream end of the M gene. This subclone, nucleotides 3693 to 3698, located in the downstream noncoding region of the P/C/D/V gene, had previously been modified into an AflIII site (TCAATC to CTTAAG) and used to accept a 63-nucleotide insert that contained a PIV3 gene-end, intergenic, and gene-start signal followed by NcoI and HindIII sites (Fig. 1A) (45). Insertion of the GFP coding sequence into this NcoI-HindIII window placed it such that it would be flanked by a set of PIV3 gene-start and gene-end signals. This subclone was then assembled into the full-length antigenomic cDNA. The total number of added nucleotides was 792, thus maintaining a final genome length that was an even multiple of six, as required for efficient RNA replication (17). rgPIV3 was rescued by cotransfecting HEp-2 cells (CCL-23; American Type Culture Collection) with the antigenomic plasmid and N, P, and L support plasmids and infecting with a recombinant modified vaccinia Ankara virus, MVA-T7, expressing T7 RNA polymerase (19). Virus stocks were further amplified in LLC-MK2 cells (CCL-7; American Type Culture Collection), and aliquots were stored at −80°C until use. rgPIV3 was found to replicate to titers similar to those obtained for the parental JS wild-type strain of PIV3 (10^8 PFU/ml). The generation of rgRSV has been reported previously (21, 22). Nonreplicating adenoviral vectors (E1a and E3 deleted) expressing GFP (AdVGFP) were obtained from the University of North Carolina (UNC) Gene Therapy Vector Core Facility as described previously (39).

HAE cell cultures. Human airway tracheobronchial epithelial cells were obtained from airway specimens resected at lung transplantation under UNC Institutional Review Board-approved protocols by the UNC Cystic Fibrosis Center Tissue Culture Core. Briefly, primary cells derived from single patient sources were expanded on plastic to generate passage 1 cells and plated at a density of 250,000 cells per well on permeable Transwell-Col (T-Col; 12-mm diameter) supports. To generate nonpolarized, poorly differentiated (PD) cells, cultures were used 2 to 4 days after seeding when subconfluent and submerged in tissue culture medium. HAE cultures were generated by provision of an ALI for 4 to 6 weeks to form well-differentiated, polarized cultures that resemble in vivo pseudostratified mucociliary epithelium as previously described (41). Cultures were derived from non-cystic fibrosis (non-CF) patients unless otherwise noted.

Viral inoculation of HAE. Frozen aliquots of rgPIV3, rgRSV, or AdVGFP were thawed immediately before use and diluted in tissue culture medium. After washing the apical surfaces of HAE with medium, 100 μl of viral suspension was applied to the apical surface for 2 h at 37°C, the inoculum was removed, and cells were returned to 37°C. Inoculation of the basolateral surface of HAE was performed by inverting the insert and exposing the basolateral surface of HAE to an equal volume and concentration of virus as used for the apical inoculations.

We utilized AdVGFP to enable expression of GFP in columnar cells of HAE as controls for transgene expression. Since we and others have previously shown that HAE is resistant to infection after lumenal inoculation of AdV unless epithelial tight junctions are disrupted, allowing access of AdV to basolateral uptake mechanisms (41, 51), we exposed the apical surfaces of HAE to sodium caprate (30 mM in tissue culture medium) for 3 min to transiently open epithelial cell tight junctions (11), followed by three phosphate-buffered saline rinses and then inoculation with AdVGFP (2×10^{10} particles [p]/ml in 300 μl of tissue culture medium for 4 h at 37°C). For all viruses, GFP expression could be detected by 20 to 24 h postinoculation (p.i.).

Photomicrographs of GFP-expressing cells were acquired using a Leica Leitz DMIRB inverted fluorescence microscope equipped with a cooled-color charge-coupled device digital camera (MicroPublisher; Q-Imaging). Quantitation of infected cells was performed with the Image Processing Tool Kit plug-ins for Photoshop (ISBN no. 1-928808-00-X; John C. Russ).

To determine the effects of neuraminidases (NAs) on rgPIV3 infection, the apical surfaces of HAE were washed with serum-free tissue culture medium and then exposed to 300 μl of the following NAs for 3 h at 37°C in serum-free tissue culture medium: *Vibrio cholerae* NA (NA III; 167 mU/ml; Sigma-Aldrich), Newcastle disease virus (Hitchner B1 strain) NA (167 mU/ml; Prozyme), and *Arthrobacter ureafaciens* NA (167 mU/ml; Prozyme). After removal of NA, the apical surfaces of HAE were rinsed in tissue culture medium before inoculation by viruses.

Immunolocalization of epithelial cell carbohydrate components and viral glycoproteins. Standard protocols were used for lectin- and antibody-based localization of target antigens on PD airway cells, HAE cultures, and histological cross-sections of HAE. Lectins were chosen that recognized specific sialic acid linkages: α2-3-linked sialic acid residues were detected with *Maackia amurensis* lectin, (MAA; EY Laboratories), and α2-6-linked sialic acid residues were detected with *Sambucus nigra* lectin (SNA; Vector Labs). Lectins were purchased conjugated to biotin linkers, and streptavidin conjugates of AlexaFluor 488 and 594 (Molecular Probes, Eugene, Oreg.) were used to detect lectin binding. For immunolocalization of HS, F58-10E4 antibody (mouse immunoglobulin M [IgM]; Seikagaku Corp.) raised against the 10E4 epitope of HS and that recognizes a heparinase-sensitive epitope on HEp-2 cells (data not shown), was incubated with PD cells on coverslips or histological cross-sections of HAE, and immunoreactivity was detected with goat anti-mouse IgM conjugated to Texas Red (Jackson ImmunoResearch).

β-Tubulin IV immunolocalization was used to identify ciliated cell types of HAE and was performed with HAE fixed with 4% paraformaldehyde (PFA). After fixation, HAE were permeabilized with 1% Triton X-100 and the apical surfaces of HAE were incubated with 10% normal goat serum prior to incubation with a β-tubulin IV monoclonal mouse IgG antibody (178 M; Sigma-Aldrich), followed by goat anti-mouse IgG conjugated to AlexaFluor 594 (Molecular Probes). Fluorescent confocal *x-z* optical sections were obtained using a Leica TCS laser scanning confocal microscope. Immunolocalization of β-tubulin IV in PFA-fixed, paraffin-embedded histological cross-sections of HAE was performed as follows: tissue sections were blocked in 3% bovine serum albumin and then probed with β-tubulin IV monoclonal mouse IgG antibody (178 M; Sigma). After washing, immunoreactivity was detected with goat anti-mouse IgG conjugated to AlexaFluor 594 (Molecular Probes).

For PIV3 F glycoprotein localization, nonpolarized human primary airway epithelial cells grown on coverslips or HAE were inoculated with rgPIV3, rgRSV, or vehicle control alone as described above and, 24 h later, cells were fixed in 4% PFA. Cells on coverslips or paraffin-embedded histological sections of HAE were probed with a monoclonal mouse IgG antibody specific for PIV3 F glycoprotein (clone 216.16), followed by goat anti-mouse AlexaFluor 594. For immunogold electron microscopy, 24 h after inoculation of HAE with rgPIV3, rgRSV, or vehicle control alone, cultures were fixed in 2% glutaraldehyde–2% PFA and incubated with 216.16 PIV3 F antibody. Immunoreactivity was detected with goat anti-mouse IgG conjugated to 12-nm colloidal gold (Jackson ImmunoResearch), and cultures were prepared and visualized using standard transmission electron microscopy techniques.

Assessment of viral shedding. Viruses released into the apical and/or basolateral compartments of HAE were harvested by the apical addition and collection of 200 μl of medium allowed to equilibrate for 30 min or by sampling 200 μl of basolateral medium. After retrieval, samples were snap-frozen on dry ice and stored at −80°C. Viral titration was performed as described previously and corrected for differences in sample volumes (16).

To investigate the morphology of HAE after rgPIV3-induced ciliated cell shedding, we compared the epithelial cell morphology of uninfected and rgPIV3-infected HAE over a 2-week period without washing of the apical surfaces. At days 2 and 13 p.i., HAE was fixed with perfluorocarbon-osmium tetroxide (a technique that preserves the hydrated state of the airway surface [50]), and prepared histological sections of the epithelium were counterstained with Richardson's stain. Transepithelial resistance was measured with a World Precision volt-ohm meter (Sarasota, Fla.) as described previously (39).

RESULTS AND DISCUSSION

Generation of rgPIV3. We used reverse genetics to engineer recombinant human PIV3 so that enhanced GFP was expressed as a separate gene placed between the P/C/D/V and M genes (Fig. 1A). The resulting recombinant virus, rgPIV3, was readily recovered and replicated in vitro with an efficiency similar to that of wild-type rPIV3 (JS strain). rgPIV3 efficiently infected and expressed GFP in HEp2 cells (Fig. 1B, panel i), A549 cells (Fig. 1B, panel ii), and primary cultures of PD, nonpolarized HAE cells (Fig. 1B, panel iii).

rgPIV3 infection of HAE occurs via the apical surface and targets ciliated epithelial cells. We then evaluated the ability of rgPIV3 to infect a well-characterized in vitro model of HAE. We inoculated the apical or basolateral surfaces of HAE with rgPIV3 (10^6 PFU; multiplicity of infection [MOI], ~3; 2 h at 37°C) and, 24 h later, quantified GFP expression as the percentage of the epithelium surface area that was positive for GFP. When administered to the apical surface, rgPIV3 infected up to 80% of the epithelium surface (Fig. 2A). For HAE derived from an individual patient, the percentage of GFP-positive epithelial surface area after rgPIV3 inoculation was dependent on the inoculum dose used (10^3 to 10^6 PFU) (data not shown). However, the maximal number of GFP-positive cells was variable between HAE derived from different patient sources, ranging from 40 to 80% of the surface area. Inoculation of the basolateral surface with rgPIV3 resulted in only occasional cells expressing GFP, with on average <0.01% of the cells GFP positive (Fig. 2B). The Transwell-Col filter support was not restrictive to permeation by rgPIV3, thus allowing access of virus to basolateral surfaces of HAE as we have also previously shown to be the case for rgRSV (53).

Confocal *x-z* optical sectioning performed 24 h p.i. revealed that HAE inoculated with rgPIV3 via the apical surface expressed GFP exclusively in columnar cells (Fig. 2C). Immunodetection of β-tubulin IV, a protein that is enriched in cilial shafts, revealed that GFP-positive cells were exclusively ciliated cell types (Fig. 2C). The differences noted above in the maximal percentages of cells that were GFP positive in HAE derived from different patients were consistent with differences

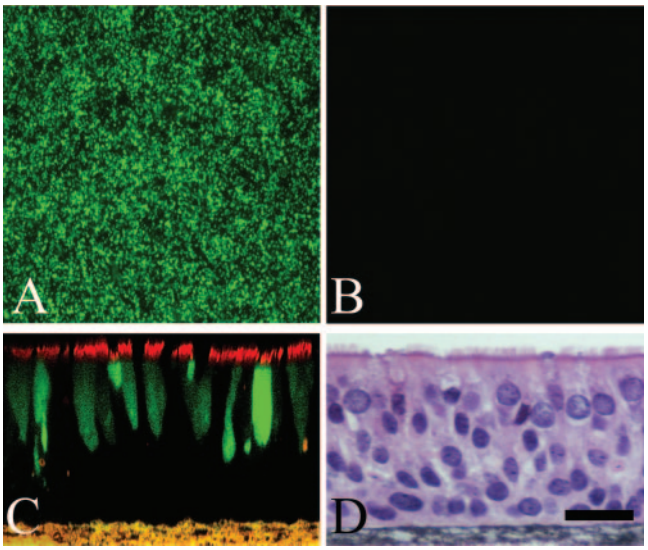

FIG. 2. Expression of GFP in HAE infected with rgPIV3 (10^6 PFU; MOI, ~3). (A and B) GFP expression in HAE viewed en face 48 h after apical (A) or basolateral (B) inoculation of HAE by rgPIV3. Original magnification, ×10. (C) Representative confocal optical section of rgPIV3-mediated GFP expression (green) in HAE 48 h following apical infection. HAE was also probed with β-tubulin IV antibody (red), revealing that GFP was present only in ciliated columnar epithelial cells. (D) Representative histological cross-section of HAE infected with rgPIV3. At 48 h p.i., no obvious cytopathic effects or cell-cell fusion was apparent. Counterstain is hematoxylin and eosin. Bar, 20 μm.

in the absolute numbers of ciliated cells in the different HAE sources. For all rgPIV3-infected HAE, there was no evidence of syncytium formation at any time point p.i. (up to 3 months) and no evidence of viral spread beyond ciliated cell types (Fig. 2C and D). The tropism of rgPIV3 for ciliated cells and the apparent absence of gross cytopathology is reminiscent of observations made with rgRSV, representing the *Pneumovirinae* subfamily of *Paramyxoviridae*, which also exclusively infects ciliated cells of HAE via the apical surface and does not result in syncytium formation (53).

Effect of HAE differentiation on susceptibility to rgPIV3 infection. Although rgPIV3 infection of HAE appeared to exclusively involve ciliated cells, PIV3 is known to efficiently infect in vitro cell cultures of nonpolarized and polarized cell lines that do not possess ciliated cell morphology (4, 5, 16, 36), as demonstrated with the nonpolarized epithelial cell lines and human PD airway epithelial cells in Fig. 1B. It therefore was of interest to monitor the susceptibility of human airway epithelial cells to infection with rgPIV3 at different stages of differentiation in vitro. In parallel, we also inoculated cells with AdVGFP, since nonpolarized human airway cells have been shown to be infected by this vector while HAE is resistant to infection via the apical surface (41). Replicate wells of HAE cells were seeded and, at various time points, the cells were inoculated with rgPIV3 (10^6 PFU; MOI, ~3) or AdVGFP (10^{10} p/ml; MOI, ~3×10^4) and GFP expression was monitored 24 h later. For rgPIV3, the susceptibility of HAE cells to infection fell into three distinct phases (Fig. 3A). During the first phase (2 to 6 days after seeding), cells displayed a PD morphology and were susceptible to infection by rgPIV3, with ~70 to 80% of the cells GFP positive when inoculated 2 days after seeding, declining to ~10% GFP-positive cells when infected at day 6. During the differentiation processes of human airway cells in vitro, days 2 to 6 after seeding represent a period of growth prior to reaching confluence and prior to polarization. An ALI environment was provided for these cultures at day 7 postseeding, which began a second phase in which susceptibility to rgPIV3 infection was reduced. During the second phase (7 to 16 days), a period when polarization and the early stages of differentiation are under way but prior to the appearance of cilia, cells were resistant to rgPIV3 infection. In the final phase (>16 days), a period when differentiation continues and ciliogenesis begins, the cultures once again became susceptible to infection by rgPIV3. Maximum susceptibility was reached ~25 days after seeding, when the airway epithelial cells have morphological features of a well-differentiated ciliated epithelium. Thus, while rgPIV3 infected only ciliated cells in HAE, airway epithelial cells that had not yet polarized or differentiated were susceptible to infection despite the

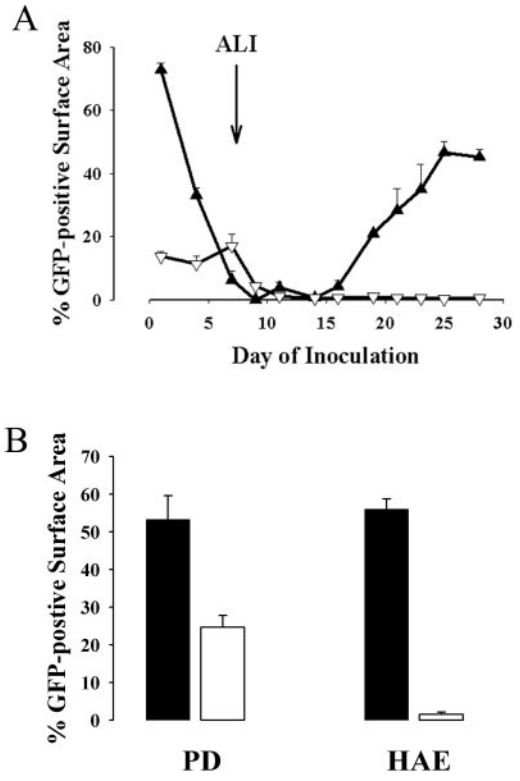

FIG. 3. Susceptibility of human airway cells to infection with rgPIV3 at various times postseeding (A) or following treatment of the lumenal surfaces of cultures with NA from *V. cholerae* (B). (A) Quantitation of GFP-positive human airway cells 24 h after inoculation of the cells with rgPIV3 (10^6 PFU) (filled triangles) or AdVGFP (10^{10} p/ml) (open triangles) at different days postseeding revealed that airway epithelial cells are initially susceptible to rgPIV3 and AdVGFP infection at early time points in culture (1 to 6 days), followed by a refractory period to both viruses that coincided with the establishment of an ALI (arrow). By 16 days, HAE regained susceptibility to infection by rgPIV3 but not AdVGFP. (B) Quantitation of GFP-positive cells present 24 h after rgPIV3 inoculation of PD airway cells or HAE either without (closed bars) or with (open bars) pretreatment of the lumenal surfaces with NA III derived from *V. cholerae* (160 mU/ml for 3 h).

absence of cilia, and on this basis were similar to monolayer cell lines. In contrast to the triphasic nature of rgPIV3 infection, AdVGFP infected nonpolarized airway epithelial cells only until they reached confluence and an ALI was initiated. At that point and for the remainder of the experiment, the cells were resistant to infection by AdVGFP.

Susceptibility of human airway epithelial cells to rgPIV3 infection following neuraminidase treatment. Infection of nonpolarized cell lines by PIV3 has been shown to be sensitive to treatment with a broad range of NAs, consistent with the idea that PIV3 attachment involves host cell sialic acid residues (29). We tested whether rgPIV3 infection of PD airway cells and HAE was sensitive to cleavage of surface sialic acid residues with *V. cholerae* NA (NA III), a broad-spectrum NA that cleaves sialic acid residues with α2–3, α2–6, and α2–8 linkages. Specifically, PD and HAE derived from the same patients were treated for 3 h with NA III and, following washing, were inoculated with 10^6 PFU of rgPIV3, and the extent of infection was assessed 24 h later (Fig. 3B). NA III treatment of HAE abolished infection by rgPIV3, whereas NA III treatment of PD cells reduced rgPIV3 infection by only ~50%, indicating that a significant proportion of infection of PD cells by rgPIV3 involved interactions insensitive to NA III treatment of the cell surface. The NA III-insensitive component of rgPIV3 infection of PD cells could reflect the presence of one or more alternative attachment-entry pathways for rPIV3 into these cells. These results are consistent with the observations of Bose et al., who reported that PIV3 infection of A549 cells was only partially sensitive to NA and was partially sensitive to heparinases, providing evidence that PIV3 infection could be mediated by sialic acid residues and/or HS moieties, at least in the A549 cell line (4).

Distribution of HS and sialic acid residues in PD airway cells and HAE. Since both HS and sialic acid residues have been implicated in mediating PIV3 infection, we investigated whether these moieties are present on the surfaces of human PD airway cells as well as in histological cross-sections of HAE cultures by using an antibody to HS and lectin probes to specific sialic acid residues (Fig. 4). First, the cells were probed with antibody F58-10E4, which is specific to HS (12). On PD airway cells, HS was detected on the surface of a subpopulation of the cells (Fig. 4A). In contrast, HS was not detected on the apical surface of HAE, but instead was detected on basal epithelial cells (Fig. 4B). Histological sections of airway epithelium derived directly from patients and probed ex vivo with F58-10E4 confirmed that HS was detectable only on basal epithelial cells (data not shown). The localization of HS on PD airway cells and on basal cells of HAE confirms earlier observations that PD cells resemble a basal cell-like phenotype that may function as progenitors to the differentiated airway epithelium (40, 42). The presence of HS on the surface of PD airway cells could provide an alternative, NA-insensitive pathway for rPIV3 attachment and infection, consistent with the evidence reported by Bose et al. with A549 cells (4). In contrast, the lack of significant apical detection of HS on HAE suggests that rgPIV3 does not use HS as a facilitator of viral infection of ciliated cells and is consistent with rgPIV3 infection of HAE being abolished by NA (Fig. 3B). Since the distribution of HS in HAE closely resembled that of airway epithelium examined ex vivo, this suggests that PIV3 infection in vivo is mediated predominantly and perhaps exclusively by an interaction with sialic acid residues, at least in the ciliated epithelium, such as is found in the nasal and sinus cavities and the conducting airways. In addition, the absence of detectable HS on the human airway surface indicates that although HS may function as a receptor surrogate for a number of diverse viruses (e.g., AdV, adeno-associated virus, and RSV), in laboratory-derived cell lines, it is likely that alternative receptors are responsible for lumenal infection of airway epithelium by these viruses. Whether HS is a requirement for infection of human alveolar regions of the lung remains to be determined. Since A549 cells are a model for alveolar epithelial cells, it is possible that PIV3 utilizes HS to facilitate infection of these regions.

We next probed PD airway cells and HAE with two lectins that discriminate between different sialic acid linkages: MAA lectin, which recognizes α2-3-linked sialic acid residues, and SNA lectin, which recognizes α2-6-linked sialic acid residues. Both lectins bound efficiently to the surface of PD cells, indicating the presence of α2-3 and α2-6 sialic acid linkages (Fig. 4C and E). Next, histological sections of HAE were probed with each lectin (Fig. 4D and F) in conjunction with antibody specific to β-tubulin IV (Fig. 4D and F) to detect and discriminate ciliated cells. Analysis with the MAA lectin showed that sialic acid residues with the α2-3 linkage were localized predominately to the apical surfaces of ciliated cells (Fig. 4D), although not all ciliated cells were positive and an occasional nonciliated cell displayed MAA binding (Fig. 4D). Analysis with the SNA lectin showed that sialic acid residues with α2-6 linkages were localized to the apical surfaces of both ciliated (Fig. 4F) and nonciliated cells, although not all ciliated or nonciliated cells were positive. Since α2-3 and α2-6 linkages were present on ciliated cells, the target cell type for rgPIV3, any of these linkages were candidates to be involved in PIV3 entry. It is noteworthy that the lectins labeled HAE predominantly on apical surfaces but for ciliated cells detection occurred predominately on the microvilli (actin-rich apical surface projections, ~2 to 3 μm in length) rather than on the membranes of the cilial shafts (tubulin-rich apical projections, 7 to 10 μm in length) per se. Of course, under the conditions of these experiments, a lack of detectable binding of lectin probes does not necessarily indicate an absence of the respective sialic acid linkage.

rgPIV3 infects ciliated cells by using a specific linkage of sialic acid residues. Since rgPIV3 infection of ciliated cells is NA sensitive but NA III cleaves a broad range of sialic acid linkages, we tested the ability of NAs that cleave a narrower spectrum of sialic acid linkages to reduce rgPIV3 infection of ciliated cells. We used rgRSV as a control for nonspecific effects of the NAs on cell viability, since NA treatment of cell lines does not affect RSV infection (2). As shown in Fig. 5A, panel ii, and B compared to the control (Fig. 5A, panel i), pretreatment of the apical surface of HAE with NA III completely inhibited rgPIV3 infection. Treatment of HAE cultures with NA derived from Newcastle disease virus that cleaves α2–3 linkages (and α2–8 linkages, although less efficiently) did not significantly reduce rgPIV3 infection of HAE (Fig. 5A, panel iii, and B). In contrast, pretreatment of the apical surfaces of HAE with NA derived from *A. ureafaciens*, which preferentially cleaves α2–6 linkages, significantly reduced rgPIV3 infection of HAE (Fig. 5A, panel iv, and B) to levels

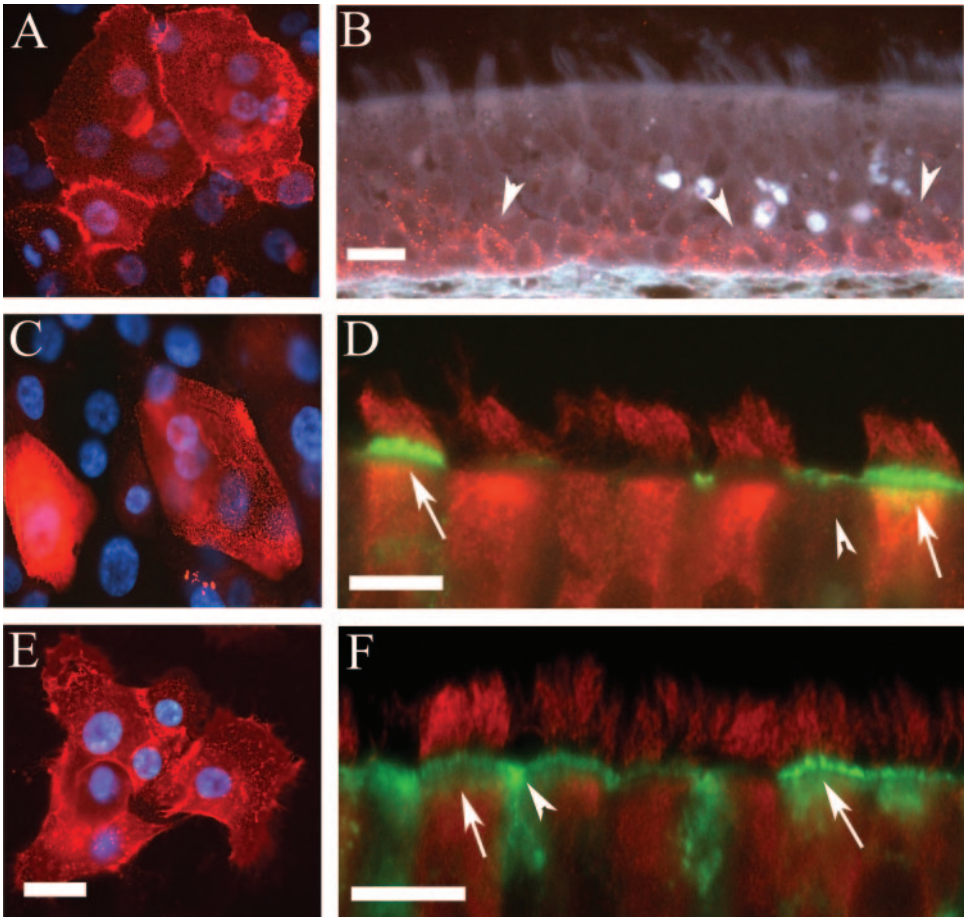

FIG. 4. Localization of cell surface HS and sialic acid linkages on PD airway cells, viewed en face (A, C, and E) and HAE, viewed in histological cross-section (B, D, and F). (A) Representative fluorescent photomicrographs of HS localization, detected with antibody F58-10E4, on the cell surface of a subpopulation of PD cells (red). (B) In HAE, HS localization was restricted to basal epithelial cells (red, arrowheads). (C and D) Sialic acid residues with α2–3 linkages, detected with MAA lectin, were present on the cell surface of a subpopulation of PD cells (C) (red), whereas in HAE (D) they were localized on the apical surface (green), viewed against a counterstain of antibody to β-tubulin IV (red). Staining with MAA was predominantly on ciliated cells (arrows in panel D) but was also detected on some nonciliated cells (arrowhead in panel D). (E and F) Sialic acid residues with α2–6 linkages, detected with SNA lectin, were present on the cell surface of PD cells (E) (red), whereas in HAE (F) localization was predominately detected on the apical surface (green), viewed against a counterstain of antibody to β-tubulin IV (red). In panel F, SNA lectin was detected on ciliated (arrows) and nonciliated (arrowheads) cells. Bar, 10 μm.

similar to that produced by NA III. Infection by rgRSV was not reduced by any of the NAs, but NA III and to a lesser extent *A. ureafaciens* NA increased the efficiency of rgRSV infection, suggesting that removal of sialic acid residues allowed improved rgRSV access to attachment and/or penetration pathways. These observations show that rgPIV3 infection of HAE ciliated cells involves predominately sialic acid residues in the α2–6 linkage. A previous study showed that PIV3 bound to purified glycolipids that displayed α2-3-linked sialic acid residues (48): our present results suggest that this in vitro activity may not be relevant to infection of HAE in vitro or in vivo.

Since our data show that α2-6-linked sialic acid residues are present on ciliated and nonciliated airway cells, the presence of the appropriate sialic acid residue apparently is not sufficient alone to account for rgPIV3 ciliated cell tropism. Sialic acid residues with α2–6 linkages have also been shown to be present on HAE examined ex vivo (3, 20) and have been associated with infection by human influenza viruses, whereas the α2–3 linkage has been associated with infection by avian influenza viruses (28). Recent results with in vitro models of HAE similar to that used in the present study indicated that human influenza viruses infected nonciliated cells and did so by an interaction with α2-6-linked sialic acid residues localized exclusively on nonciliated cells (33). Whether human influenza viruses infect human ciliated cells, as does rgPIV3, in our model of HAE remains to be determined, although the rapid and extensive cell destruction noted previously for HAE infected by influenza A virus suggests that these predominately ciliated cell cultures are highly susceptible to infection by these viruses (53). In addition, it is unclear why SNA lectin only recognized nonciliated cells in the studies of Matrosovich et al., while our data show SNA recognition of both ciliated and nonciliated cells with functional enzymatic data showing α2-6-linked sialic acid residues mediating infection of ciliated cells by rgPIV3. Analysis of cell type infection by human and avian influenza viruses in our model of HAE may reveal that, if

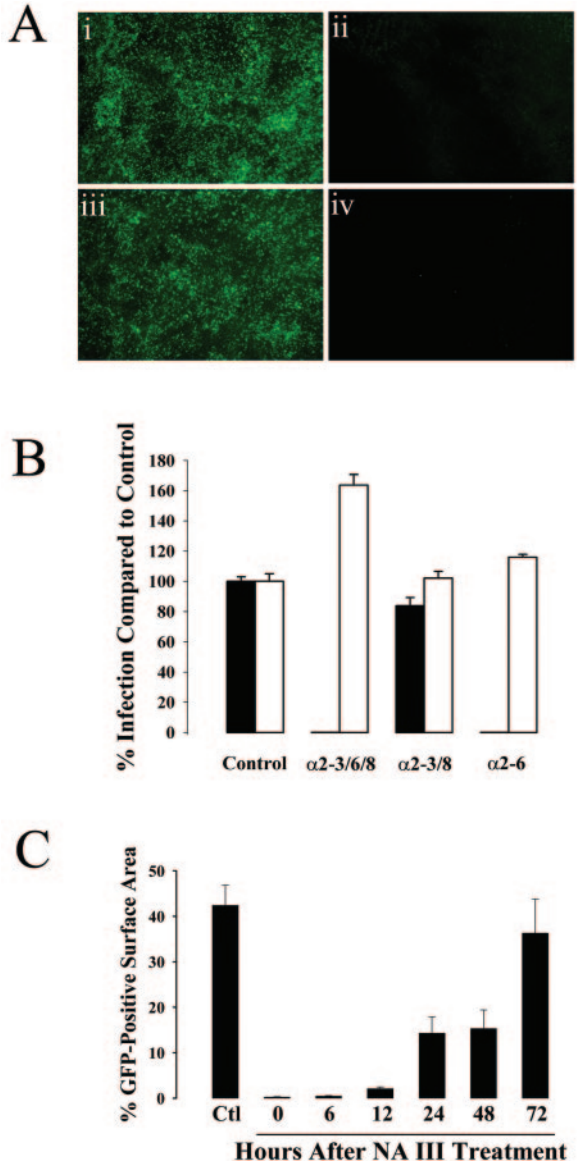

FIG. 5. Inhibition of rgPIV3 infection of HAE following lumenal treatment with NAs from different organisms. (A) Representative en face photomicrographs of HAE exposed to vehicle control alone (i) or treated with NA from *V. cholerae*, which cleaves α2–3, -6, and -8 linkages (ii); Newcastle disease virus NA, specific for α2–3 and α2–8 linkages (iii); or *A. ureafaciens* NA, which is specific for α2–6 linkages. NAs were applied to the apical surface for 3 h immediately prior to washing and inoculation with rgPIV3. GFP-positive cells were photographed 24 h later. (B) Quantitation of GFP expression from experiments such as shown in panel A, representing cultures from three different patients, each in duplicate. Cultures of HAE were treated with the NAs described above (shown as sialic acid linkages cleaved, with the control being vehicle alone) and infected with rgPIV3 (filled bars) or rgRSV (open bars). The expression of GFP was quantified 24 h p.i. The data shown represent means ± standard errors (SE) of the GFP-positive surface area. (C) Recovery of susceptibility to infection with rgPIV3 following treatment with *V. cholerae* NA III that cleaves α2–3, -6, and -8 linkages. Replicate cultures of HAE were treated on the apical surface with NA III for 3 h, and the apical surface was inoculated with rPIV3 immediately (0 h) or following 6, 12, 24, 48, or 72 h of recovery. A control culture (Ctl) was infected without prior NA III treatment. The expression of GFP was quantified 24 h p.i. The data shown represent means ± SE of the GFP-positive surface area from duplicate cultures derived from two different patient samples.

different from the previous study, HAE grown under different conditions can lead to altered glycosylation profiles of cell surface glycoconjugates.

We next measured the time required for NA III-treated HAE to recover susceptibility to infection by rgPIV3. Replicate cultures of HAE were treated with NA III, washed, incubated at 37°C and, at intervals, inoculated with rgPIV3. The extent of infection was measured at 24 h p.i. (Fig. 5C). Restoration of rgPIV3 susceptibility to infection required 24 to 72 h. These data indicate that the NA III-sensitive cell components that facilitate rgPIV3 infection are only slowly replenished. Previous studies have shown that replenishment of sialic acid following surface desialylation depends on de novo glycoprotein synthesis, although a subset of specific molecules can be resialylated by recycling through the *trans*-Golgi compartment (24). The half-time of surface resialylation has been reported to be 12 to 16 h (43), which contrasts with the much slower rate of recovery (half-time, ~48 to 72 h) described here.

rgPIV3-expressed F glycoprotein accumulates in membranes of cilial shafts. Infection of permissive nonpolarized cell cultures with PIV3 typically results in cell-cell fusion and the formation of multinucleated syncytia, mediated by the surface expression of the HN and F glycoproteins and their interactions with the membranes of neighboring cells (37). Given the lack of syncytium formation with rgPIV3-infected ciliated cells of HAE, we examined the localization of rgPIV3 F glycoprotein in PD airway cells and ciliated cells of HAE by immunodetection with an F-specific PIV3-neutralizing mouse monoclonal antibody (216.16). Examination of rgPIV3-infected PD airway cells 24 h p.i. revealed that F was distributed in a nonpolarized manner and was visualized primarily at the cell edges, reflecting accumulation at the cell surface (Fig. 6A, panel i). A similar distribution is observed for monolayer cultures of cell lines such as LLC-MK2 and makes F available for contact and fusion with neighboring cells (data not shown).

In contrast, F glycoprotein expressed in rgPIV3-infected HAE was localized exclusively to the apical surface of ciliated cells (Fig. 6A, panel ii). The accumulation of F glycoprotein exclusively on the apical surface of ciliated cells and the presence of tight junctions in these cells would restrict the F glycoprotein from interacting with the plasma membranes of adjacent cells. This could account for the absence of syncytium formation in HAE, as has also been suggested for polarized cells infected with RSV (44, 53). The lack of syncytium formation in HAE in vitro corresponds well with the rarity of syncytia in pathological specimens of paramyxovirus-infected HAE in vivo (1). These observations also suggest that the role of the F glycoprotein is to allow fusion of the virus with host cell membranes, thus mediating infection rather than a having a role in mediating cell-cell fusion. However, the potential impact of cell-cell fusion mediated by F glycoprotein in the nonconducting airway alveolar regions was not tested in this study. Reproducible in vitro models of human primary alveolar epithelium that retain the morphological and functional characteristics of the human alveoli are not yet available to test this hypothesis. Interestingly, most of the F glycoprotein in HAE was located in regions corresponding to the membranes of the cilial shafts, although some F was also possibly localized to the microvillus regions of ciliated cells (Fig. 6A, panel iii). Transmission electron microscopy with the same anti-F monoclonal antibody

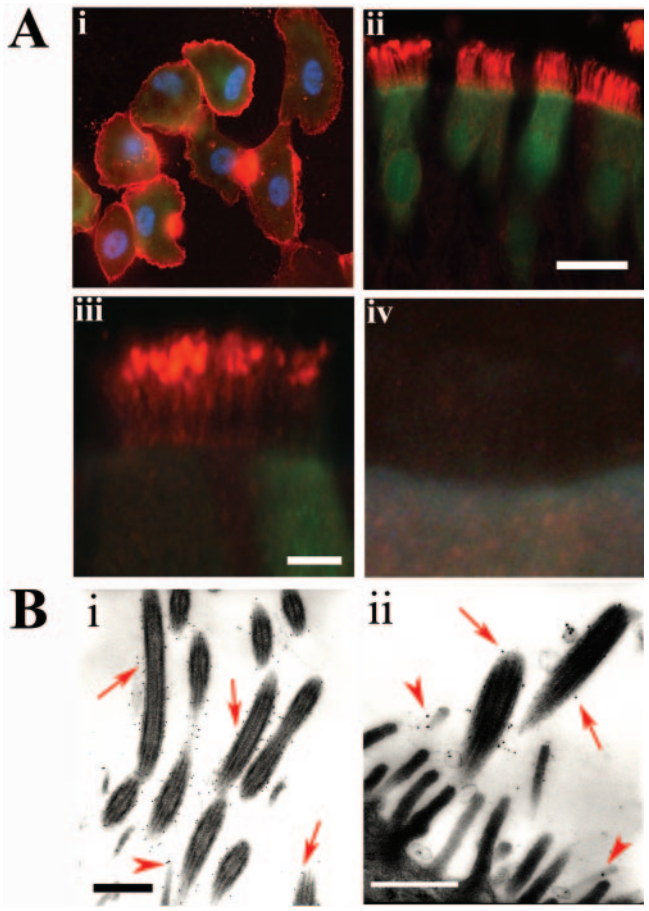

FIG. 6. Localization of the PIV3 F glycoprotein in rgPIV3-infected PD airway cells and HAE. (A) Photomicrographs of PD airway cells viewed en face (i) and HAE in histological cross-sections (ii, iii, and iv). The cells were infected with rgPIV3 (i, ii, and iii) or rgRSV (iv), incubated for 24 h, and stained with a monoclonal antibody specific to the F glycoprotein (red). The F glycoprotein was localized in the surface membrane of PD airway cells (i) and in the membranes of the cilial shafts of HAE (ii and iii). No immunoreactivity for PIV3 F glycoprotein was detected with rgRSV-inoculated cultures probed under identical conditions to those described above (iv). Bars, 10 μm (ii) or 3 μm (iii and iv). (B) Electron transmission photomicrographs of the apical surface of rgPIV3-infected HAE cells, probed with a monoclonal antibody specific to the F glycoprotein and detected with an immunogold secondary antibody (12 nm). Immunoreactivity to F glycoprotein was localized predominantly to membranes of the cilial shafts (arrows in panels i and ii) and occasionally in ciliated cell microvilli projections (arrowheads in panels i and ii). No immunogold was observed in rgRSV-infected HAE or in HAE inoculated with vehicle control alone and probed with antibodies under identical conditions to those described above (data not shown). Bars, 0.2 μm.

conjugated to immunogold confirmed that F was localized predominately to the upper membranous regions of the cilial shafts (Fig. 6B). This strongly suggests that virus budding and shedding may occur from the cilial shafts per se. It is noteworthy that Sendai virus entry and release have been shown to be associated with the membranes of the cilial shafts in explants of guinea pig trachea (15). In the present paper, lectin staining indicated that α2-6-linked sialic acid was predominately associated with apical structures distinct from the cilia (Fig. 4F). This raises the possibility that the sites of PIV3 entry and budding might be distinct. However, it also is possible that the cilia contain α2-6-linked sialic acid in quantities sufficient for viral attachment but below the limit of detection by lectins.

The possibility that rgPIV3 may bud from the cilial shaft membranes is an intriguing observation, since it has been reported that enveloped viruses, including the paramyxoviruses, favor budding from cholesterol-rich membrane regions commonly referred to as lipid rafts (6, 30, 38). Molecules that have glycophosphatidyl-inositol (GPI)-linked structures have been well documented to favor the lipid raft environment, and proteins isolated from the primary cilium of paramecium were exclusively GPI linked (7, 8). In addition, we have previously shown using a viral overexpression model that GPI-linked proteins are trafficked to the apical surface of ciliated cells and tend to accumulate in the upper membranous regions of the cilial shaft (46). Thus, we suggest that PIV3 budding occurs in regions corresponding to lipid rafts that are components of the cilial shaft membranes. PIV3 budding has previously been associated with the cytoskeletal protein tubulin, and it is noteworthy that cilial shafts contain significant quantities of β-tubulin IV (Fig. 2).

rgPIV3 is shed from the apical surface of ciliated cells, and viral spread is facilitated by coordinated ciliary beat. Since infected ciliated cells traffic F glycoproteins to the apical surface, we tested whether ciliated cell budding and release of virus was also restricted to the apical compartment of HAE. The apical surfaces of HAE were inoculated with rgPIV3 (10^6 PFU), and supernatants were collected separately from apical or basolateral compartments each day for 12 days. Using standard titration assays on HEp-2 cells, significant amounts of rgPIV3 ($\sim 5 \times 10^5$ to 2×10^7 PFU/culture) were detected in samples harvested from the apical surfaces of HAE, reaching a maximum titer of 2×10^7 PFU/culture after 2 days of infection (data not shown). Viral shedding gradually decreased to 5×10^5 PFU/culture by 12 days p.i. No virus was detected from basolateral samples, with a detection limit of 10 PFU.

Thus, rgPIV3 infection, viral assembly, and shedding occurred exclusively via the apical surfaces of ciliated airway epithelial cells. In polarized A549 cells, PIV3 also shed predominately from the apical surface but, in addition, was detected in the basolateral compartments (5). For ciliated cells it is possible that trafficking of viral components is more tightly regulated and, as a consequence, viral budding occurs exclusively at the apical surface. We have not performed similar studies with primary cell models of human alveolar cells, and the pattern of viral shedding in this lung epithelial cell type might be different from the pattern of shedding in ciliated epithelial cells derived from the conducting airways. We previously reported that the spread of rgRSV infection in HAE was facilitated by coordinated cilial beat (53). The coordinated directional movement of lumenal secretions (as an index of mucociliary transport) in HAE cultures is an interesting facet of this airway culture model (35). Furthermore, the altered homeostatic ion transport mechanisms associated with CF lung disease lead to reduced airway surface liquid volume on the apical surface, reduced cilial beat or function, and decreased mucociliary transport, all of which are reflected in HAE derived from CF airway cells (34). We therefore compared rgPIV3 infection of non-CF and CF HAE to investigate the

role of cilial beat in the spread of the virus and to examine the effect of CF physiological defects on infection.

Initially, to determine whether non-CF and CF HAE are equally infected by rgPIV3, we inoculated the apical surfaces of non-CF and CF HAE with a high inoculum of rgPIV3 (10^6 PFU). As shown in Fig. 7A and B, there was no difference in the ability or efficiency of rgPIV3 to infect HAE derived from non-CF and CF sources. We also did not detect any differences in the relatively nonpathogenic nature of the infection. To monitor rgPIV3 spread, non-CF and CF HAEs were inoculated with a low inoculum of rgPIV3 (10^3 PFU) (Fig. 7C and D). For both non-CF and CF HAEs, low numbers of cells were GFP positive at 1 day p.i., confirming that non-CF and CF HAEs were equally susceptible to infection by rgPIV3. By 2 days p.i., for non-CF HAE increasing numbers of GFP-positive cells were apparent, indicating efficient spread of progeny virions. In addition, the directional pattern of viral spread suggested facilitation by the movement of cilial beat (Fig. 7E). By 3 days p.i., the infection was homogenously distributed throughout the surface of the cultures (Fig. 7G). For CF HAE, although infection was similar on day 1 p.i., the extent and pattern of infection on days 2 and 3 p.i. indicated that rgPIV3 did not spread as efficiently in CF HAE as in non-CF HAE (Fig. 7F and H). For CF HAE, rosette-like patterns surrounding an initial foci of infection were observed, whereas infection of non-CF HAE produced a directional and, later, a homogenous infection. This suggests that spread of rgPIV3 in CF HAE was limited to those cells closely juxtaposed to the cells producing progeny virus. Therefore, coordinated cilial beat in HAE appeared to facilitate spread of rgPIV3 from ciliated cell to ciliated cell, a process that is hindered by conditions of compromised mucociliary transport, such as occurs in CF lung disease.

Loss of rgPIV3-mediated GFP expression over time is due to shedding of ciliated cells. The resolution of PIV3 infection in vivo most likely occurs via a combination of innate and adaptive immunity directed at both the virus and the virus-infected cells of the airway. Since the HAE model is devoid of immune cell-mediated innate and adaptive immunity mechanisms as well as neutralizing antibodies, this model can be used to determine the epithelium-based innate immune responses that may limit the extent and duration of viral infection. To determine the duration of rgPIV3 infection of ciliated cells, we inoculated HAE with rgPIV3 (10^6 PFU) and assessed GFP expression over a 4-week time period. As shown in Fig. 8A, GFP expression peaked at 2 days p.i., followed by a rapid decline in the numbers of GFP-positive cells until a low but persistent level (0.01% of cells) was achieved by 7 days p.i. In contrast, inoculation of HAE with AdVGFP (an infection that was dependent on first disrupting the tight junctions with sodium caprate) resulted in similar numbers of columnar cells expressing GFP at 2 days p.i. However, the rate of loss of AdV-mediated GFP-positive cells was less than that for rgPIV3, with ~50% of the maximum number of GFP-positive cells remaining positive at 30 days p.i. The rapid loss of GFP-positive cells observed after rgPIV3 infection compared to that with AdVGFP coincided with the appearance of increased numbers of floating cells in the apical surface secretions of HAE compared to AdVGFP-infected or uninfected HAE. This suggested that the rgPIV3-infected cells were shed from the epithelium, although we cannot rule out additional concurrent

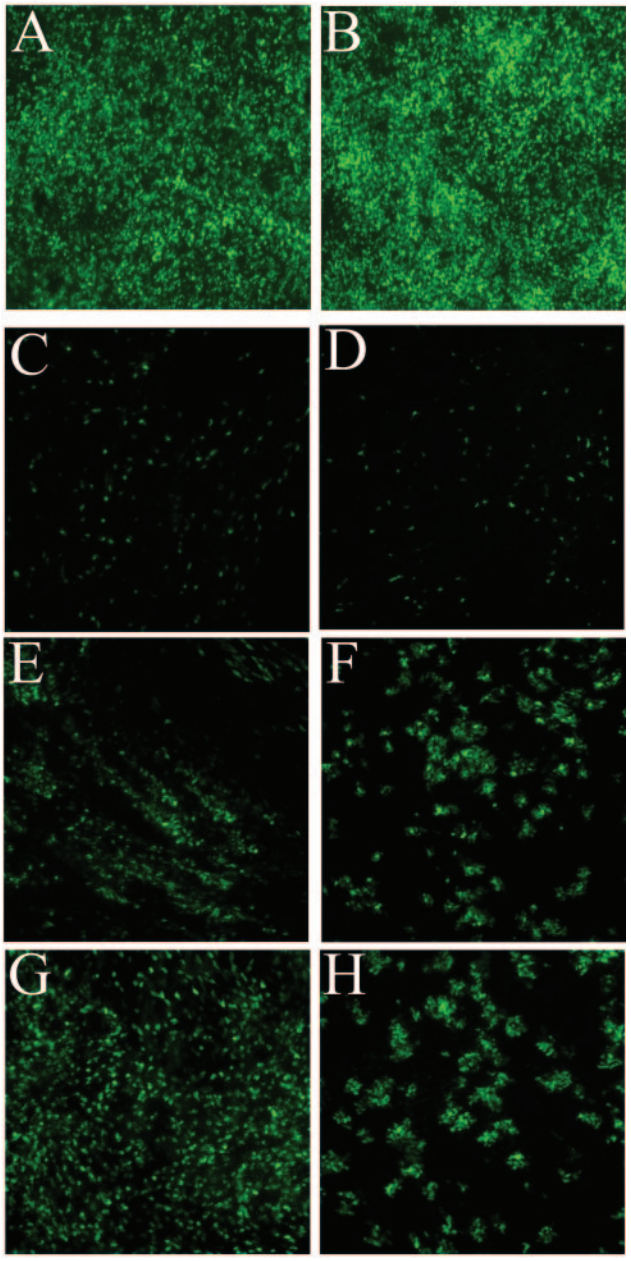

FIG. 7. Spread of rgPIV3 infection is compromised in HAE derived from CF airway epithelium. rgPIV3-mediated expression of GFP viewed en face in HAE derived from a non-CF patient (A, C, E, and G) and from a CF patient (B, D, F, and H). Inoculation of the apical surfaces of non-CF (A) or CF (B) HAE with a high titer of rgPIV3 (10^6 PFU) resulted in similar levels of infection at 24 h p.i. Similarly, with a low-titer rgPIV3 inoculum (10^3 PFU), lower but comparable numbers of GFP-positive cells were detected 24 h after inoculation in non-CF (C) and CF (D) HAE. Following the pattern of viral spread with time revealed that viral spread was facilitated by coordinated cilial beat in non-CF HAE by 48 h p.i. (E), leading to homogenous distribution of infection by 72 h (G). In contrast, for CF HAE, viral spread was restricted to cells in close proximity to the primary infected cells and spread remained limited at both 48 (F) and 72 (H) h p.i. Original magnification, ×10.

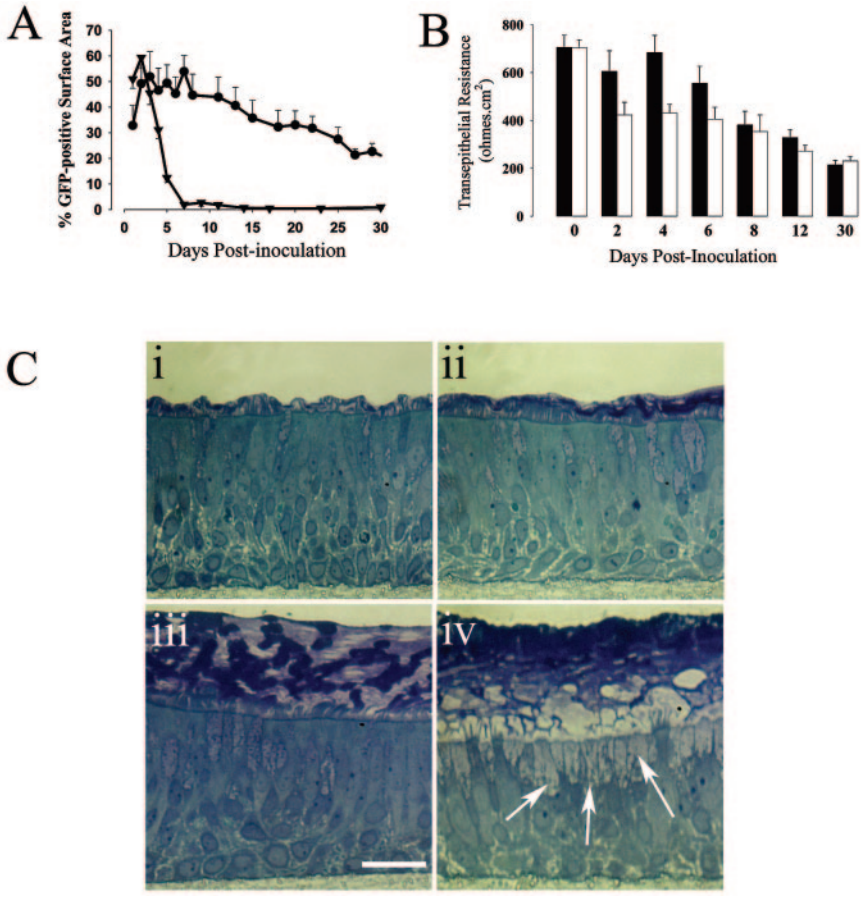

FIG. 8. rgPIV3-induced ciliated cell shedding leads to mucin-containing cell metaplasia in HAE. (A) Quantitation of the percentage of GFP-positive cells over time after apical inoculation of HAE with rgPIV3 (10^6 PFU; closed triangles) or AdVGFP (10^{10} p/ml; inoculated after sodium caprate treatment to open epithelial tight junctions; closed circles). (B) Transepithelial resistance measurements over time after inoculation of HAE with rgPIV3 (open bars) or vehicle control only (filled bars). (C) Representative histological sections of perfluorocarbon-osmium tetroxide-fixed HAE inoculated with either vehicle control (i and iii) or rgPIV3 (ii and iv) and fixed 2 days p.i. (i and ii) or 13 days p.i. (iii and iv). Note the increased presence of mucin-containing cells (indicated by arrows) in HAE inoculated with rgPIV3 and fixed 13 days p.i. Bar, 20 μm.

mechanisms for the loss of GFP-containing cells. The loss of ciliated cells from HAE did not adversely affect the integrity of the epithelium on the basis of gross inspection or the loss of maintenance of an ALI. Measurement of the transepithelial resistance after rgPIV3 infection revealed that there was a small decrease on days 2 to 6 p.i. compared to the uninfected control, but overall the resistance for infected HAE remained similar to control cultures and was consistent with maintenance of a tight epithelium (Fig. 8B). This is noteworthy because the maintenance of resistance depends on the integrity of the epithelium, and it raised the possibility that the loss of large numbers of rgPIV3-infected ciliated cells might occur through some orderly host mechanism, such as acceleration of normal ciliated cell turnover, rather than through disorderly cell destruction by virus-induced mechanisms.

Histological examination of rgPIV3-infected HAE on day 13 p.i., a time subsequent to the loss of most of the GFP-expressing cells, revealed that the morphology had been transformed from that of a normal ciliated epithelium (Fig. 8C, panel i) into one that was rich in mucin-containing cells and lacking in ciliated cells (Fig. 8C, panel iv). In contrast, uninfected controls retained the normal predominately ciliated morphology after 13 days (Fig. 8C, panel iii). Mucin-containing cell metaplasia leading to increased mucus production in the airways has been noted in infants with respiratory virus infections and has generally been, in part, considered to be the result of epithelial cell damage produced by host cell-mediated immune responses directed against virus-infected cells (10). The present results suggest an alternative hypothesis: namely, that the mucin-containing cell metaplasia indeed is a consequence of the extensive loss of ciliated cells, although this loss is not obligatorily due to host immune mechanisms, but instead represents an epithelial cell response to infection. This might involve an acceleration of the normal mechanism whereby ciliated cells are shed. Apoptosis in response to virus infection is one candidate to be the trigger for the accelerated shedding. Metaplasia of mucin-containing cells might represent an intermediate condition where ciliated cell replacement has not kept up with loss, or it might have functional significance on its own and could be part of the program of lung recovery.

In summary, using a model of human ciliated airway epithelium, we have shown that a recombinant respirovirus, rgPIV3, exclusively infected ciliated airway epithelial cells of the lumenal airway surface. Infection of ciliated cells by rgPIV3 de-

pended on α2-6-linked sialic acid residues, which were located mainly on the apical surface of ciliated cells, but was not detected in abundance on cilia. The PIV3 F glycoprotein trafficked to the apical surface and predominantly to membranes of the cilial shafts, suggesting that the cilial shaft membranes are the regions from which progeny viruses bud. The polarized accumulation of the F glycoprotein likely limits its access to membranes of neighboring cells and likely explains the lack of syncytium formation in this model and perhaps in PIV3 infection of conducting airway epithelium in vivo. Progeny viruses were shed exclusively from the apical surface, and the spread of infection followed the directional movement of the cilial beat. Most of the rgPIV3-infected cells appeared to be shed from the apical surface within several days, although the integrity of the epithelium remained intact overall. We speculate that rgPIV3 infection caused an acceleration in the mechanism for the turnover of lumenal ciliated epithelial cells. The loss of ciliated cells was associated with a mucin-containing cell metaplasia, which appears to be an intermediate in the epithelial response to infection.

Models of HAE such as the one reported here will be useful for the study of virus-epithelial cell interactions in the human lung and determination of the pathophysiological consequences of viral infection of HAE, since infection and cytotoxicity can be assessed in the absence of cell-mediated immune responses that complicate interpretation of in vivo observations. The specificity of rgPIV3 for the ciliated epithelial cell, combined with its ability to readily accommodate and express foreign inserts (45), makes this virus an attractive tool for studying the delivery of transgenes to human ciliated airway cells. Since the airway epithelial cell types considered to require correction in CF airways are the ciliated airway epithelial cells, the ability of PIV3 to target ciliated cells may be important for the further development of corrective gene transfer strategies for CF lung disease.

ACKNOWLEDGMENTS

This work was supported by NIH/NHLBI HL 51818-09, HL 66943-01, and a Cystic Fibrosis Foundation research grant (L.Z.).

We also thank the directors and teams of the UNC CF Center Tissue Culture Core, the Molecular Core, the Morphology and Morphometry Core, the UNC Gene Therapy Vector Core, and the Michael Hooker Microscopy Facility for supplying reagents and technical expertise.

REFERENCES

1. **Aherne, W., T. Bird, S. Court, et. al.** 1970. Pathological changes in virus infections of the lower respiratory tract in children. J. Clin. Pathol. **23:**7–18.
2. **Barretto, N., L. K. Hallak, and M. E. Peeples.** 2003. Neuraminidase treatment of respiratory syncytial virus-infected cells or virions, but not target cells, enhances cell-cell fusion and infection. Virology **313:**33–43.
3. **Baum, L. G., and J. C. Paulson.** 1990. Sialyloligosaccharides of the respiratory epithelium in the selection of human influenza virus receptor specificity. Acta Histochem. Suppl. **40:**35–38.
4. **Bose, S., and A. K. Banerjee.** 2002. Role of heparan sulfate in human parainfluenza virus type 3 infection. Virology **298:**73–83.
5. **Bose, S., A. Malur, and A. K. Banerjee.** 2001. Polarity of human parainfluenza virus type 3 infection in polarized human lung epithelial A549 cells: role of microfilament and microtubule. J. Virol. **75:**1984–1989.
6. **Campbell, S. M., S. M. Crowe, and J. Mak.** 2001. Lipid rafts and HIV-1: from viral entry to assembly of progeny virions. J. Clin. Virol. **22:**217–227.
7. **Capdeville, Y.** 2000. Paramecium GPI proteins: variability of expression and localization. Protist **151:**161–169.
8. **Capdeville, Y., and A. Benwakrim.** 1996. The major ciliary membrane proteins in Paramecium primaurelia are all glycosylphosphatidylinositol-anchored proteins. Eur. J. Cell Biol. **70:**339–346.
9. **Chanock, R. M., B. R. Murphy, and P. L. Collins.** 2001. Parainfluenza viruses, p. 1341–1380. *In* D. M. Knipe and P. M. Howley (ed.), Fields virology, 4th ed., vol. 1. Lippincott Williams & Wilkins, Philadelphia, Pa.
10. **Collins, P. L., R. M. Chanock, and B. R. Murphy.** 2001. Respiratory syncytial virus, p. 1443–1485. *In* D. M. Knipe and P. M. Howley (ed.), Fields virology, 4th ed., vol. 1. Lippincott Williams & Wilkins, Philadelphia, Pa.
11. **Coyne, C. B., M. M. Kelly, R. C. Boucher, and L. G. Johnson.** 2000. Enhanced epithelial gene transfer by modulation of tight junctions with sodium caprate. Am. J. Respir. Cell. Mol. Biol. **23:**602–609.
12. **David, G., X. M. Bai, B. Van der Schueren, J. J. Cassiman, and H. Van den Berghe.** 1992. Developmental changes in heparan sulfate expression: in situ detection with mAbs. J. Cell Biol. **119:**961–975.
13. **Dechecchi, M. C., P. Melotti, A. Bonizzato, M. Santacatterina, M. Chilosi, and G. Cabrini.** 2001. Heparan sulfate glycosaminoglycans are receptors sufficient to mediate the initial binding of adenovirus types 2 and 5. J. Virol. **75:**8772–8780.
14. **Dechecchi, M. C., A. Tamanini, A. Bonizzato, and G. Cabrini.** 2000. Heparan sulfate glycosaminoglycans are involved in adenovirus type 5 and 2-host cell interactions. Virology **268:**382–390.
15. **Dourmashkin, R., and D. L. Tyrrell.** 1970. Attachment of two myxoviruses to ciliated epithelial cells. J. Gen. Virol. **9:**77–88.
16. **Durbin, A. P., S. L. Hall, J. W. Siew, S. S. Whitehead, P. L. Collins, and B. R. Murphy.** 1997. Recovery of infectious human parainfluenza virus type 3 from cDNA. Virology **235:**323–332.
17. **Durbin, A. P., J. W. Siew, B. R. Murphy, and P. L. Collins.** 1997. Minimum protein requirements for transcription and RNA replication of a minigenome of human parainfluenza virus type 3 and evaluation of the rule of six. Virology **234:**74–83.
18. **Feldman, S. A., S. Audet, and J. A. Beeler.** 2000. The fusion glycoprotein of human respiratory syncytial virus facilitates virus attachment and infectivity via an interaction with cellular heparan sulfate. J. Virol. **74:**6442–6447.
19. **Fuerst, T. R., E. G. Niles, F. W. Studier, and B. Moss.** 1986. Eukaryotic transient-expression system based on recombinant vaccinia virus that synthesizes bacteriophage T7 RNA polymerase. Proc. Natl. Acad. Sci. USA **83:**8122–8126.
20. **Gagneux, P., M. Cheriyan, N. Hurtado-Ziola, E. C. van der Linden, D. Anderson, H. McClure, A. Varki, and N. M. Varki.** 2003. Human-specific regulation of alpha 2-6-linked sialic acids. J. Biol. Chem. **278:**48245–48250.
21. **Hallak, L. K., P. L. Collins, W. Knudson, and M. E. Peeples.** 2000. Iduronic acid-containing glycosaminoglycans on target cells are required for efficient respiratory syncytial virus infection. Virology **271:**264–275.
22. **Hallak, L. K., D. Spillmann, P. L. Collins, and M. E. Peeples.** 2000. Glycosaminoglycan sulfation requirements for respiratory syncytial virus infection. J. Virol. **74:**10508–10513.
23. **Heminway, B. R., Y. Yu, and M. S. Galinski.** 1994. Paramyxovirus mediated cell fusion requires co-expression of both the fusion and hemagglutinin-neuraminidase glycoproteins. Virus Res. **31:**1–16.
24. **Hoe, M. H., P. Slusarewicz, T. Misteli, R. Watson, and G. Warren.** 1995. Evidence for recycling of the resident medial/trans Golgi enzyme, N-acetylglucosaminyltransferase I, in ldlD cells. J. Biol. Chem. **270:**25057–25063.
25. **Krusat, T., and H. J. Streckert.** 1997. Heparin-dependent attachment of respiratory syncytial virus (RSV) to host cells. Arch. Virol. **142:**1247–1254.
26. **Lamb, R., and D. Kolakofsky.** 1996. Paramyxoviridae: the viruses and their replication, p. 1305–1340. *In* D. M. Knipe and P. M. Howley (ed.), Fields virology, 4th ed., vol. 1. Lippincott Williams & Wilkins, Philadelphia, Pa.
27. **Lamb, R. A.** 1993. Paramyxovirus fusion: a hypothesis for changes. Virology **197:**1–11.
28. **Lamb, R. A., and R. M. Krug.** 2001. *Orthomyxoviridae*: the viruses and their replication, p. 1487–1579. *In* D. M. Knipe and P. M. Howley (ed.), Fields virology, 4th ed., vol. 1. Lippincott, Williams and Wilkins, Philadelphia, Pa.
29. **Levin Perlman, S., M. Jordan, R. Brossmer, O. Greengard, and A. Moscona.** 1999. The use of a quantitative fusion assay to evaluate HN-receptor interaction for human parainfluenza virus type 3. Virology **265:**57–65.
30. **Manie, S. N., S. Debreyne, S. Vincent, and D. Gerlier.** 2000. Measles virus structural components are enriched into lipid raft microdomains: a potential cellular location for virus assembly. J. Virol. **74:**305–311.
31. **Markwell, M. A., and J. C. Paulson.** 1980. Sendai virus utilizes specific sialyloligosaccharides as host cell receptor determinants. Proc. Natl. Acad. Sci. USA **77:**5693–5697.
32. **Markwell, M. A. K., P. Fredman, and L. Svennerholm.** 1984. Receptor ganglioside content of three hosts for Sendai virus MDBK, HeLa, and MDCK cells. Biochim. Biophys. Acta **775:**7–16.
33. **Matrosovich, M. N., T. Y. Matrosovich, T. Gray, N. A. Roberts, and H. D. Klenk.** 2004. Human and avian influenza viruses target different cell types in cultures of human airway epithelium. Proc. Natl. Acad. Sci. USA **101:**4620–4624.
34. **Matsui, H., B. R. Grubb, R. Tarran, S. H. Randell, J. T. Gatzy, C. W. Davis, and R. C. Boucher.** 1998. Evidence for periciliary liquid layer depletion, not abnormal ion composition, in the pathogenesis of cystic fibrosis airways disease. Cell **95:**1005–1015.
35. **Matsui, H., S. H. Randell, S. W. Peretti, C. W. Davis, and R. C. Boucher.**

1998. Coordinated clearance of periciliary liquid and mucus from airway surfaces. J. Clin. Investig. **102:**1125–1131.
36. **Moscona, A.** 1997. Interaction of human parainfluenza virus type 3 with the host cell surface. Pediatr. Infect. Dis. J. **16:**917–924.
37. **Moscona, A., and R. W. Peluso.** 1992. Fusion properties of cells infected with human parainfluenza virus type 3: receptor requirements for viral spread and virus-mediated membrane fusion. J. Virol. **66:**6280–6287.
38. **Nguyen, D. H., and J. E. Hildreth.** 2000. Evidence for budding of human immunodeficiency virus type 1 selectively from glycolipid-enriched membrane lipid rafts. J. Virol. **74:**3264–3272.
39. **Pickles, R., J. Fahrner, J. Petrella, R. Boucher, and J. Bergelson.** 2000. Retargeting the coxsackievirus and adenovirus receptor to the apical surface of polarized epithelial cells reveals the glycocalyx as a barrier to adenovirus-mediated gene transfer. J. Virol. **74:**6050–6057.
40. **Pickles, R. J., P. M. Barker, H. Ye, and R. C. Boucher.** 1996. Efficient adenovirus-mediated gene transfer to basal but not columnar cells of cartilaginous airway epithelia. Hum. Gene Ther. **7:**921–931.
41. **Pickles, R. J., D. McCarty, H. Matsui, P. J. Hart, S. H. Randell, and R. C. Boucher.** 1998. Limited entry of adenovirus vectors into well-differentiated airway epithelium is responsible for inefficient gene transfer. J. Virol. **72:** 6014–6023.
42. **Randell, S. H.** 1992. Progenitor-progeny relationships in airway epithelium. Chest **101:**11S–16S.
43. **Reichner, J. S., S. W. Whiteheart, and G. W. Hart.** 1988. Intracellular trafficking of cell surface sialoglycoconjugates. J. Biol. Chem. **263:**16316–16326.
44. **Roberts, S. R., R. W. Compans, and G. W. Wertz.** 1995. Respiratory syncytial virus matures at the apical surfaces of polarized epithelial cells. J. Virol. **69:** 2667–2673.
45. **Skiadopoulos, M. H., S. R. Surman, J. M. Riggs, C. Orvell, P. L. Collins, and B. R. Murphy.** 2002. Evaluation of the replication and immunogenicity of recombinant human parainfluenza virus type 3 vectors expressing up to three foreign glycoproteins. Virology **297:**136–152.
46. **Stonebraker, J., D. Wagner, R. W. Lefensty, K. Burns, S. J. Gendler, J. Bergelson, R. C. Boucher, W. K. O'Neal, and R. J. Pickles.** 2004. Glycocalyx restricts adenoviral vector access to apical receptors expressed on respiratory epithelium in vitro and in vivo: role for tethered mucins as barriers to lumenal infection. J. Virol. **78:**13755–13768.
47. **Summerford, C., and R. J. Samulski.** 1998. Membrane-associated heparan sulfate proteoglycan is a receptor for adeno-associated virus type 2 virions. J. Virol. **72:**1438–1445.
48. **Suzuki, T., A. Portner, R. A. Scroggs, M. Uchikawa, N. Koyama, K. Matsuo, Y. Suzuki, and T. Takimoto.** 2001. Receptor specificities of human respiroviruses. J. Virol. **75:**4604–4613.
49. **Takimoto, T., G. L. Taylor, H. C. Connaris, S. J. Crennell, and A. Portner.** 2002. Role of the hemagglutinin-neuraminidase protein in the mechanism of paramyxovirus-cell membrane fusion. J. Virol. **76:**13028–13033.
50. **Tarran, R., B. R. Grubb, D. Parsons, M. Picher, A. J. Hirsh, C. W. Davis, and R. C. Boucher.** 2001. The cf salt controversy. In vivo observations and therapeutic approaches. Mol. Cell **8:**149–158.
51. **Walters, R. W., T. Grunst, J. M. Bergelson, R. W. Finberg, M. J. Welsh, and J. Zabner.** 1999. Basolateral localization of fiber receptors limits adenovirus infection from the apical surface of airway epithelia. J. Biol. Chem. **274:** 10219–10226.
52. **Yao, Q., X. Hu, and R. W. Compans.** 1997. Association of the parainfluenza virus fusion and hemagglutinin-neuraminidase glycoproteins on cell surfaces. J. Virol. **71:**650–656.
53. **Zhang, L., M. Peeples, R. Boucher, P. Collins, and R. J. Pickles.** 2002. Respiratory syncytial virus infection of human airway epithelial cells is polarized, specific to ciliated cells, and without obvious cytotoxicity. J. Virol. **76:** 5654–5666.